



**HAL**  
open science

# Polycyclic aromatic hydrocarbons containing heavy group 14 elements: From synthetic challenges to optoelectronic devices

Thomas Delouche, Muriel Hissler, Pierre-Antoine Bouit

## ► To cite this version:

Thomas Delouche, Muriel Hissler, Pierre-Antoine Bouit. Polycyclic aromatic hydrocarbons containing heavy group 14 elements: From synthetic challenges to optoelectronic devices. *Coordination Chemistry Reviews*, 2022, 464, pp.214553. 10.1016/j.ccr.2022.214553 . hal-03638218

**HAL Id: hal-03638218**

**<https://hal.science/hal-03638218>**

Submitted on 12 Apr 2022

**HAL** is a multi-disciplinary open access archive for the deposit and dissemination of scientific research documents, whether they are published or not. The documents may come from teaching and research institutions in France or abroad, or from public or private research centers.

L'archive ouverte pluridisciplinaire **HAL**, est destinée au dépôt et à la diffusion de documents scientifiques de niveau recherche, publiés ou non, émanant des établissements d'enseignement et de recherche français ou étrangers, des laboratoires publics ou privés.

## Review

# Polycyclic aromatic hydrocarbons containing heavy Group 14 elements: from synthetic challenges to optoelectronic devices

Thomas Delouche, Muriel Hissler, Pierre-Antoine Bouit  
Univ Rennes, CNRS, ISCR - UMR 6226, F-35000 Rennes.

Email(s): pierre-antoine.bouit@univ-rennes1.fr

---

**Abstract:** Polycyclic aromatic hydrocarbons (PAHs) are important organic building blocks for optoelectronic applications. Among the various molecular engineering strategies ( $\pi$ -extension, edge structure modification, exocyclic functionalization), this review will focus on the insertion of heavy group 14 elements (Si, Ge and Sn) into the polyaromatic backbone. The main synthetic approaches toward these compounds will be discussed. Their optical and redox properties will be described with a particular attention of the specific effect of the heteroatom. Finally, their insertion into optoelectronic devices will be highlighted.

**Keywords:** Polycyclic aromatic hydrocarbons – Silicon – Germanium - Tin – Optical properties – Redox properties – Optoelectronic devices.

---

## Contents

|   |    |
|---|----|
| I Introduction                            | 1  |
| 2 PAHs containing 5-membered heterocycles | 4  |
| 3 PAHs containing 6-membered heterocycles | 10 |
| 4 PAHs containing 7-membered heterocycles | 16 |
| 5 Conclusion                              | 18 |
| Declaration of Competing Interest         | 18 |
| Acknowledgements                          | 18 |
| References                                | 19 |

## I. Introduction

Polycyclic aromatic hydrocarbons, usually denominated through their abbreviation PAHs, are molecules constituted of  $sp^2$  hybridized C atoms organized in ortho- and peri-fused aromatic rings.<sup>1</sup> When larger than one nanometer, they are often called

nanographenes.<sup>2</sup> These  $\pi$ -conjugated systems proved during the last 20 years their efficiency as semi-conductors in various applications (Organic Field-Effect Transistors (OFETs), Organic Solar Cells (OSCs), organic batteries ...). Different synthetic strategies have been developed to modify their molecular structure and thus their electronic properties and device performances. The first is to increase the size of the  $\pi$ -systems from the prototypic hexaperibenzocoronene **1** (Fig. 1) to Graphene Nanoribbons (GNR).<sup>3</sup> A second strategy is to modify the C-*sp*<sup>2</sup> skeleton by introducing various ring-sizes (5, 6 or 7-membered rings such in **2**, Fig. 1).<sup>4</sup> In addition to the modification of  $\pi$ -delocalization and self-assembly, this strategy allows preparing chiral PAHs (the so called chiral nanographenes).<sup>5</sup> Finally, another strategy consists of tuning the edge configuration.<sup>6</sup> While introducing fjord configuration also allows preparing chiral PAHs, the introduction of zigzag edges configurations allows stabilizing open shell diradicaloid such **3** (Fig. 1). All these strategies rely on the modification of the C-based skeleton. However, an alternative approach is to selectively replace C-atoms by heteroatoms.<sup>7</sup> For example, during the last decade, this approach was successfully applied to triels (B<sup>8</sup>), pnictogens (N,<sup>9</sup> and P<sup>10</sup>) or chalcogens (O<sup>11</sup>, S<sup>12</sup>) (compounds **4-7**, Fig. 1) and even recently to heavier main group elements.<sup>13</sup>

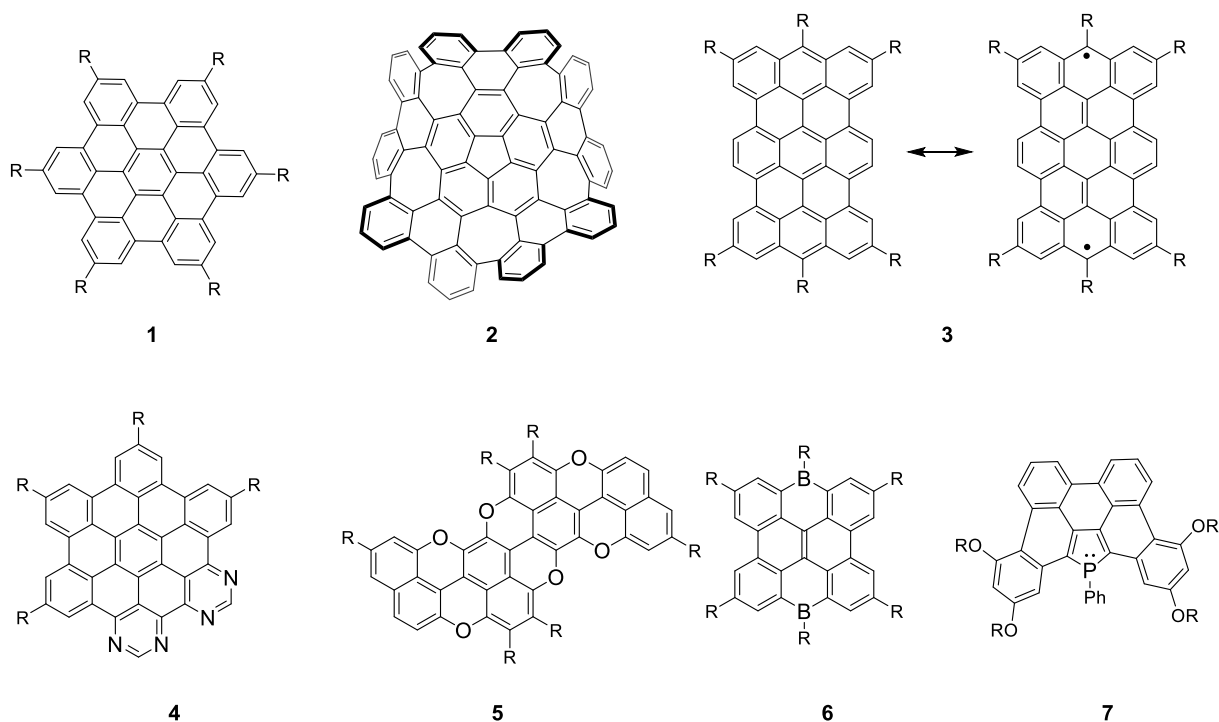


**Figure 1:** Examples of planar(**1**), contorted (**2**), open-shell (**3**) and heteroatoms containing PAHs (**4-7**)

Despite the “vertical analogy” with carbon, there are surprisingly few examples of PAHs containing heavy Group 14 elements, which is somehow surprising considering the important role played by  $\pi$ -conjugated siloles (Fig. 2) in opto-electronic applications such OSCs or Organic-Light-Emitting Diodes (OLEDs).<sup>14</sup> Hence, siloles display a general property in Group 14 metalloles: they possess a low lying lowest unoccupied molecular orbital (LUMO) due to hyperconjugation between the  $\sigma^*$ -orbitals of the exocyclic ER bonds (E = Si, Ge, Sn) and a  $\pi^*$ -orbital of the dienic system.<sup>15</sup> As a consequence, such metalloles display red-shifted absorptions and

lowest reduction potential than the corresponding cyclopentadiene.<sup>16</sup> In addition, hexaphenyl-siloles became one of the flagship compounds of the Aggregation-Induced Emission (AIE) literature and their intense light emission in the condensed phase was used in various applications (from biology to material science).<sup>17</sup> Following these observations, various  $\pi$ -conjugated oligomers and polymers, were prepared mainly containing siloles, but also germoles and stannoles (**8-9**, Fig. 2).<sup>18,19,20,21</sup> However, many group-14 containing  $\pi$ -systems are only used as precursors for the corresponding B-containing compounds, (for example the B-acenes).<sup>22</sup> On the other hand, the field of Pb-containing  $\pi$ -systems is almost unexplored, mainly because of the weakness of Pb–C bonds.<sup>23-24</sup> In addition, organosilicon derivatives offer the possibility to prepare stable compounds displaying unusual electronic configurations (either high-<sup>25</sup> or low-coordination number<sup>26</sup> or  $\pi$ -single bonding<sup>27</sup>). All these peculiar properties make them valuable building blocks for  $\pi$ -conjugated system engineering.

In this article, we will focus on PAHs incorporating Si, Ge or Sn atoms, their synthesis, the impact of the heteroatoms on the electronic properties, and their insertion in optoelectronic devices. As the definition of PAHs varies depending on the articles, we decided to limit this review to compounds featuring heterocycles that are ortho- and peri-fused and featuring at least 14 C- $sp^2$  atoms in the  $\pi$ -conjugated framework. This thus excludes ortho-fused PAHs such linear hetero-acenes and -helicenes, which were previously reviewed.<sup>28</sup> Bridged triarylsilanes<sup>29</sup> and heterofluorenes<sup>18</sup> will not be covered by this review either. All along this review, a particular focus will be devoted to the description of the synthetic approaches, as obtaining such derivatives often represents a synthetic challenge. This is classical with PAHs, but here PAHs chemistry has to be combined with the specificity of organo-main group elements, that usually display high reactivity due to large bond lengths and poor orbital overlap.

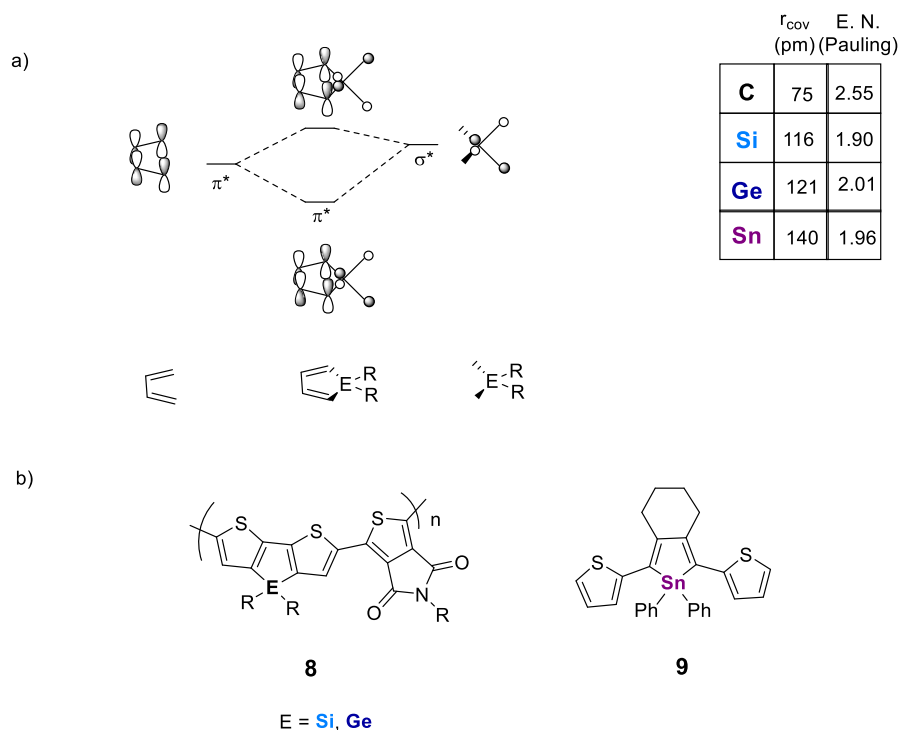
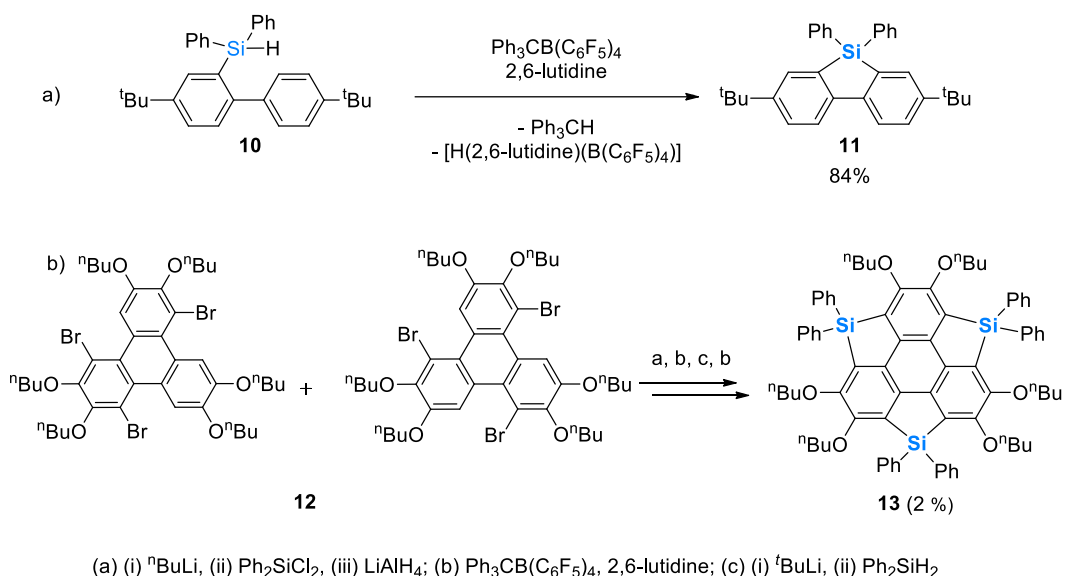


**Figure 2:** a) Partial MO description of group 14 metalloles (E = Si, Ge, Sn); b) example of  $\pi$ -conjugated siloles, germoles and stannoles<sup>30</sup>

## II. PAHs containing 5-membered heterocycles

As mentioned in the introduction, the most widely studied class of tetrel containing  $\pi$ -systems are by far the metalloles. Such heterocycle are usually prepared through lithiation-substitution, it is thus normal that this methodology has been widely used to introduce these subunits into PAHs. However, as we will see interesting alternative approaches have also been proposed recently.

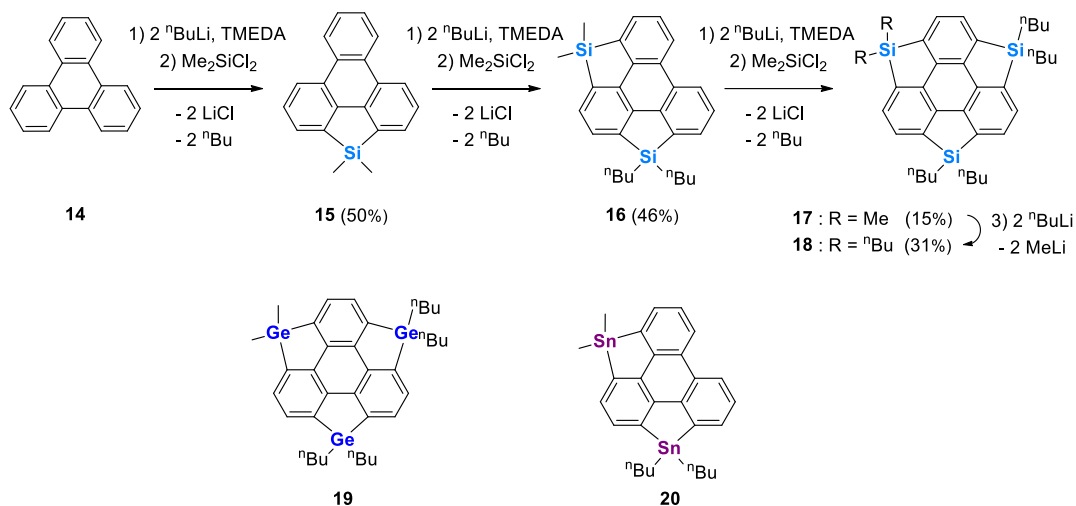
In 2009, Kawashima and coworkers developed a sila-Friedel-Crafts reaction toward dibenzosilole **11** (Scheme 1a) that they further applied to the synthesis of trisilasumanene **13**.<sup>31</sup> While sumanenes and trithiasumanenes display a concave  $\pi$ -surface, **13** is planar, as evidenced by its crystallographic structure (Fig. 4). This planarization is explained by the longer distances of the C–Si bonds compared to C–C or C–S bonds. The insertion of the three siloles in the structure of **13** is accompanied by the appearance in the UV-vis absorption of a weak transition at low energy ( $\lambda > 365$  nm) compared to its triphenylene analogue. As expected due to its rigid polyaromatic framework, **13** is fluorescent ( $\lambda_{em} = 427$  nm) in diluted dichloromethane solution ( $c = 2.10^{-5}$  M). Interestingly, it is also luminescent in solid-state ( $\lambda_{em} = 447$  nm).<sup>32</sup>



### Scheme 1: Sila-Friedel-Crafts approach to trisilasumanene **13**

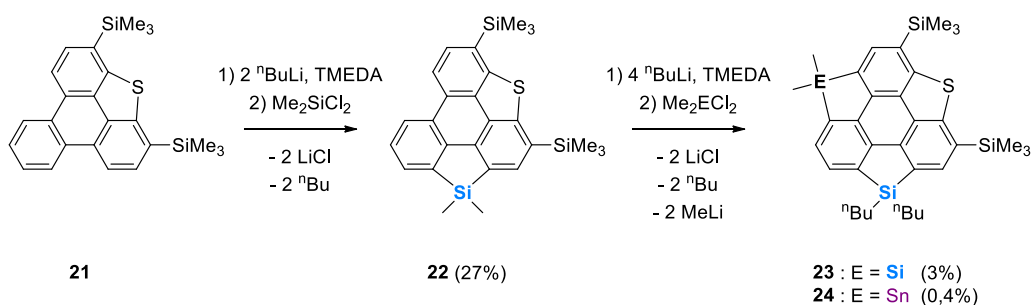
At the same period, Saito and coworkers developed a stepwise lithiation of the bay region of triphenylenes that offer an alternative strategy toward trisilasumanenes (Scheme 2).<sup>33,34</sup> The authors could isolate the intermediates and thus study the effect of successive insertion of siloles on the optical properties. Despite the expected  $\sigma^*-\pi^*$  conjugation in the LUMO, typical of metalloles, an almost neglectable redshift has been observed ( $\Delta\lambda_{abs}^{max}(\mathbf{14}\text{-}\mathbf{18}) = 8$  nm). However, this redshift is larger in emission, as a consequence of a more important reorganization in the excited state. Such observation is not intuitive as **14** and **18** have both fully planar and rigid framework. Interestingly, the blue-shift between **13** and **18** ( $\Delta\lambda_{em} = 47$  nm) points out the major role played by the electron rich exocyclic alkoxy groups of **13**. The same synthetic approach allowed the authors to prepare the trigermasumanene **19**.<sup>35</sup> As previously observed in metallole oligomers, **18** and **19** display similar absorption/emission properties.

The authors also applied this strategy to form triphenylenodistannole **20** (Fig. 4) in low yield (9%). Tristannasumanene could not be observed, presumably because of competition between lithiation and cleavage of the Sn–C bonds. The optical properties are similar to the similar derivatives with Si (**16**) ( $291 \text{ nm} < \lambda_{\text{abs}} < 292 \text{ nm}$ , DCM,  $c \sim 10^{-5} \text{ M}$ ).<sup>35</sup>



**Scheme 2:** Direct lithiation approach toward heterasumanenes **17-20**

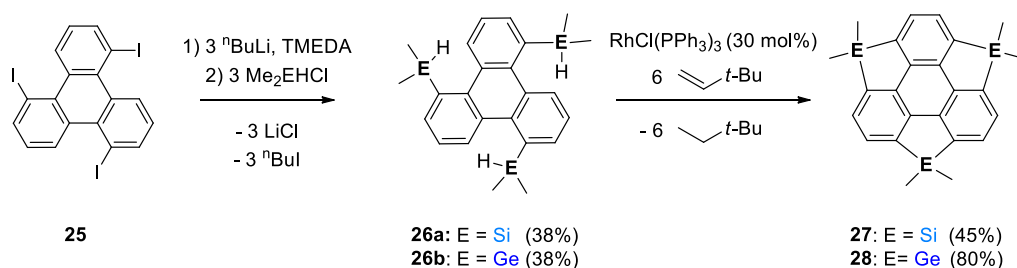
Finally, using their lithiation method, Saito's group could also prepare in very low yield heterasumanenes **22-24** featuring different heteroatoms starting from triphenylenothiophene **21** (Scheme 3).<sup>36</sup> At that time, this was the first synthetic approach toward heterasumanenes featuring two or three different heteroatoms. Nevertheless, no optical properties are reported in the article.



**Scheme 3:** Synthesis of heterasumanenes **23-24** with 2 or 3 different heteroatoms

More recently, Xu and coworkers developed a Rh-catalysed approach to trisilasumanene and trigermasumanene through a threefold cyclodehydrogenation of Si/Ge–H and C–H bonds (Scheme 4).<sup>37</sup> One advantage of this strategy is to avoid the multiple lithiation steps described previously which led to poor yields. Similarly to its Si analogue **27**, **28** adopts a planar structure (Fig. 4). They also confirmed Saito's observation on the weak impact of changing the tetrel in heterasumanene, as **27-28** display similar absorption/emission properties (Fig. 3). The electronic properties were also studied by density functional theory (DFT) calculations. Such computational studies are of prime importance in metalloles in order to evaluate the involvement of

E in the FMOs. Here, authors show that while the highest occupied molecular orbital (HOMOs) of sumanene ( $E = \text{CH}_2$ ), **27** and **28** are similar, their LUMOs are delocalized over the entire hetero-polyaromatic skeleton, indicating the  $\sigma^*-\pi^*$  conjugations of the metaloles. Calculations also predict a lower gap for **27** compared to **28**, which is not reflected in the experimental spectroscopic data. Recently, Xu group also demonstrated that iodine-doped sumanene can be used as intermediates for the preparation of heterasumanenes such **23**.<sup>38</sup>



**Scheme 4:** Rh-catalysed approach to heterasumanenes **27-28**

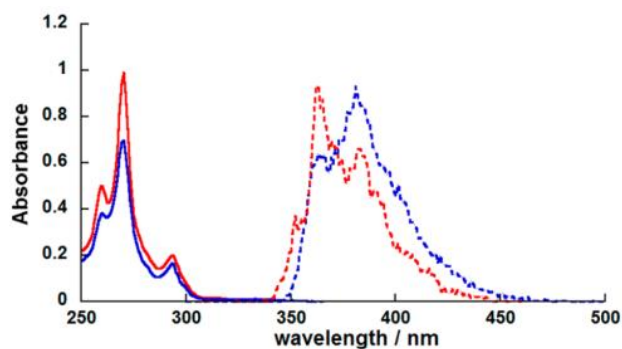


**Figure 3:** UV-Absorption (solid line) and emission (dashed line) spectra of **27** (blue) and **28** (red) in diluted dichloromethane (DCM,  $c \sim 10^{-5}$  M). Reprinted with permission from ref 37.

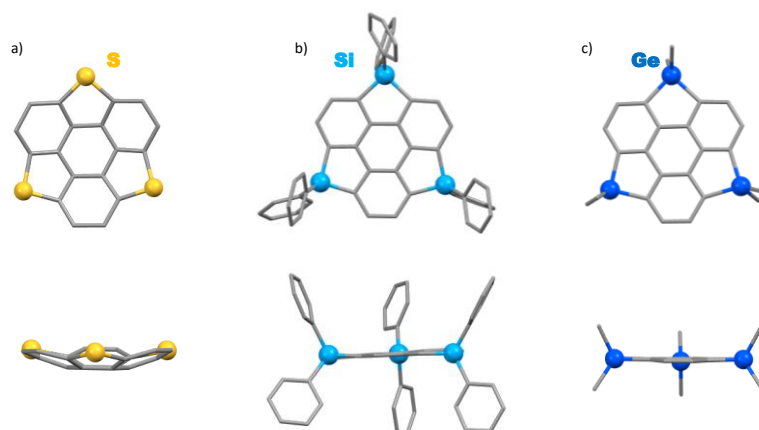
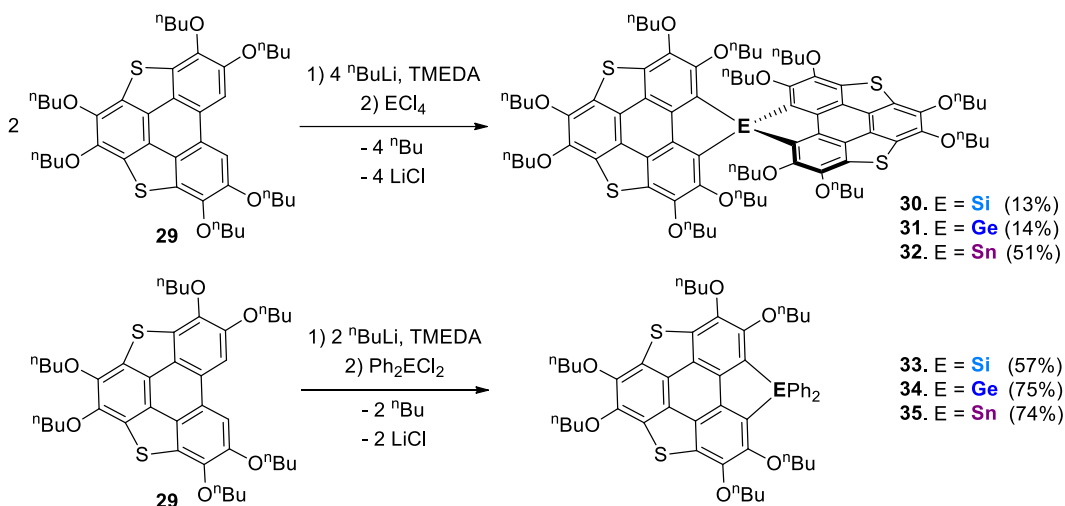


**Figure 4:** X-ray structures of trithiasumanene (a), trisilasumanene **13** (b) (butyloxy groups omitted for clarity) and trigermasumanene **28** (c).

Finally, Saito and coworkers recently took advantage of the specific ability of heavy group 14 elements to form spiro derivatives.<sup>39</sup> The synthesis of **30-32** was achieved with low yield using their direct-lithiation strategy (Scheme 5). In the key step, they used  $\text{ECl}_4$  (E = Si, Ge, Sn) as tetrel source for the formation of the spiro derivatives. For comparison, they also prepared in good yields the corresponding non-spiro derivatives **33-35**. The two planar PAHs backbones of **30-32** were almost perpendicular (dihedral angles between  $85^\circ$  and  $89^\circ$ ) as evidenced by X-ray crystallography and DFT calculations (Fig. 5).



**Scheme 5:** Synthesis of (spiro)-heterasumanenes **30-35**

UV-vis absorption spectra (DCM,  $c = 10^{-5}$  M) of the spiro-type **30-32** showed slightly longer absorption maxima (with  $\lambda_{\text{max}} \sim 400\text{-}403$  nm) compared to the non-spiro compounds **33-35** (390—397 nm). The FMOs give insight into this phenomenon as the LUMOs are stabilized through  $\sigma^*-\pi^*$  conjugation thus leading to extended conjugation between the PAHs in the spiro forms (Fig. 5). The non-spiro **33-35** display only one reversible oxidation in cyclic voltammetry (CV) at +0.40 V vs  $\text{Fc}^+/\text{Fc}$ . The spiro **30-32** show two reversible oxidation waves, with the first potential being in the same range than the non-spiro analogue (+0.40 V vs  $\text{Fc}^+/\text{Fc}$ ). This can be explained by looking at the FMOs as HOMO / HOMO-1 do not show orbital contributions from the heteroatom (Fig. 5). In all cases, the potential seems independent of the heteroatom. Additional DFT calculations suggest the presence of spiro-conjugation in the LUMO between the orthogonal PAHs bridged by group 14 atoms (Fig. 5).



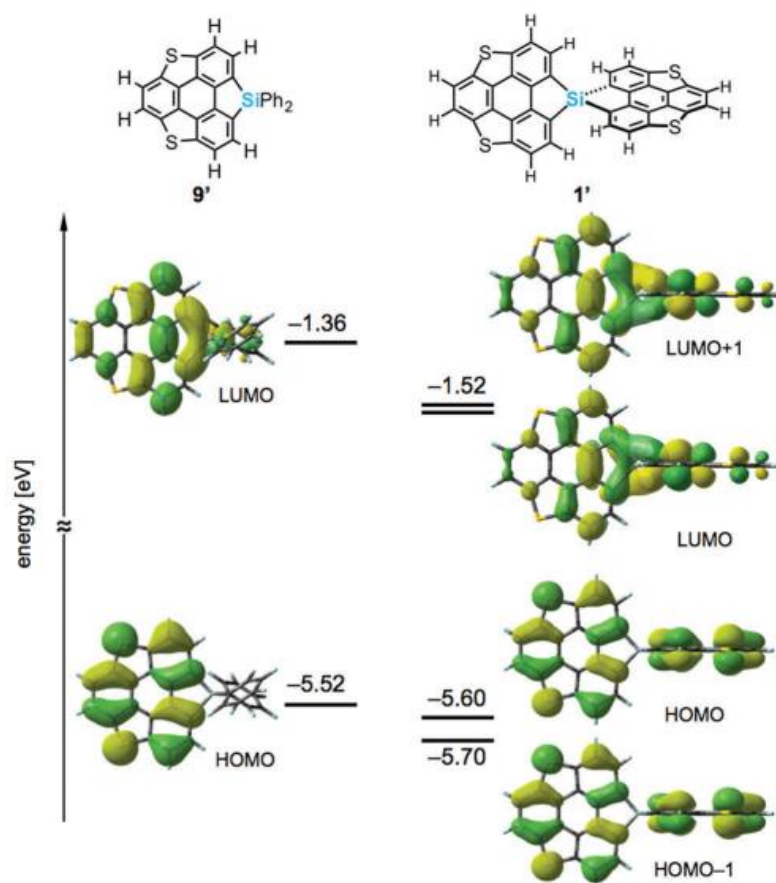
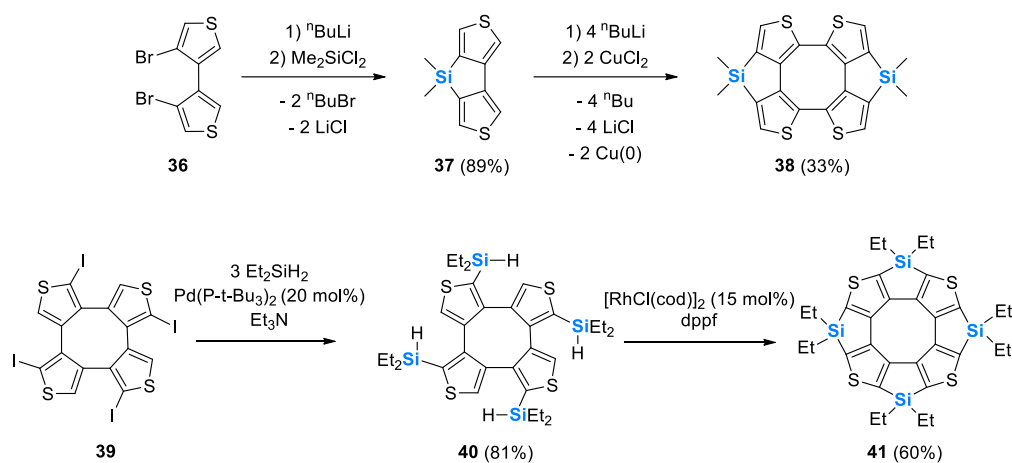


**Figure 5:** DFT calculated (B3LYP/6-31G(d)) frontier molecular orbitals of **30**. Reprinted with permission from ref 39.

Iyoda and coworkers described the synthesis of cyclic tetrathiophenes planarized by silyl groups **38** (Scheme 6).<sup>40</sup> This was achieved in moderate yield through the Cu-mediated coupling of dithienosiloles **37**. Contrary to its S-analog, the presence of the Si bridges does not fully planarize the central cyclooctatetraene (COT) unit, due to longer Si-C bonds compared to the S-C bond. Hence, the structure displays some distortion (Fig. 6). However, the COT ring displays a high degree of antiaromaticity according to Nucleus Independent Chemical Shift (NICS(0) = +12.7). The UV-vis absorption spectrum of **38** ( $\lambda_{\text{abs}} = 483 \text{ nm}$ ) is considerably red-shifted compared to its non silylated analogue which is colourless ( $\lambda_{\text{abs}} = 335 \text{ nm}$ ), as a result of a better planarization. In addition to the oxidation wave at +0.45 V vs Fc<sup>+</sup>/Fc, which is present in the non silylated analogue, **38** displays two reversible reduction waves ( $E_{\text{red}}^1 = -2.09 \text{ V}$  vs Fc<sup>+</sup>/Fc). Likewise, the radical cation **38**<sup>•+</sup>, radical anion **38**<sup>•-</sup> and dianion **38**<sup>2-</sup> could be characterized by electron paramagnetic resonance and UV-Vis absorption. In diluted DCM solution, the longest absorption maxima of **38**<sup>•+</sup> (at) and **38**<sup>•-</sup> were observed respectively in the near infrared (1178 nm) and the visible (766 nm) respectively.



**Scheme 6:** Synthesis of disilatetraphia[8]circulene **38** and tetrasilatetraphia[8]circulene **41**

[8]circulenes are currently attracting lot of attention in the field of novel aromatics.<sup>41</sup> During their work on hetero[8]circulenes,<sup>42</sup> Miyake and coworkers reported the preparation of the first tetrasilatetraphia[8]circulene **41**.<sup>43</sup> This silane fragment was introduced by mean of Pd-catalysed silylation of iodo-precursor **39** (Scheme 6). The [8]circulene **41** was then constructed through fourfold Rh-catalysed dehydrogenative silylation in excellent yield. As evidenced by its X-ray structure (Fig. 6), **41** is almost planar with the central eight-membered ring being a regular octagon. **41** is more easily oxidized ( $E_{ox} = +0.74$  V vs  $Fc^+/Fc$ ) than its non silylated analogue ( $E_{ox} = +1.31$  V vs  $Fc^+/Fc$ ) due to better conjugation in the planar **41**. Similarly, a red shift in UV-Vis absorption is observed for **41** with a longest absorption wavelength at 341 nm in DCM. However, such absorption are blue shifted compared to fully carbonated [8]circulene despite their  $\pi$ -curvature.<sup>41</sup> Of particular interest, an efficient intersystem crossing takes place at low temperature with the appearance of phosphorescence at low energy ( $\lambda_{fluo} = 397$  nm;  $\lambda_{phos} = 548$  nm). The same team later reported the Ge-containing analogue of **41** using a similar synthetic approach.<sup>44</sup> In this case, the HOMO-LUMO gap appeared larger than the Si-congener, but the optical properties are not strongly affected, even if the authors could observe differences in the excited state dynamics.

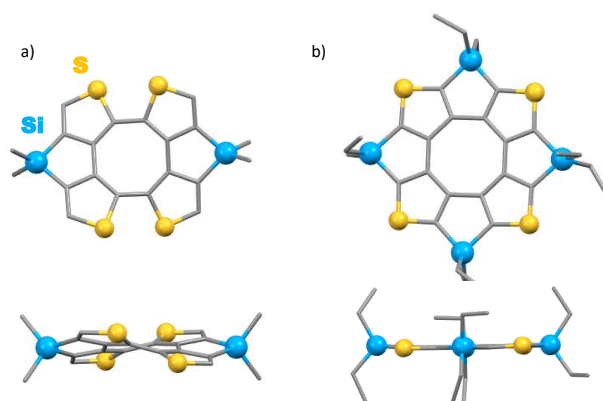
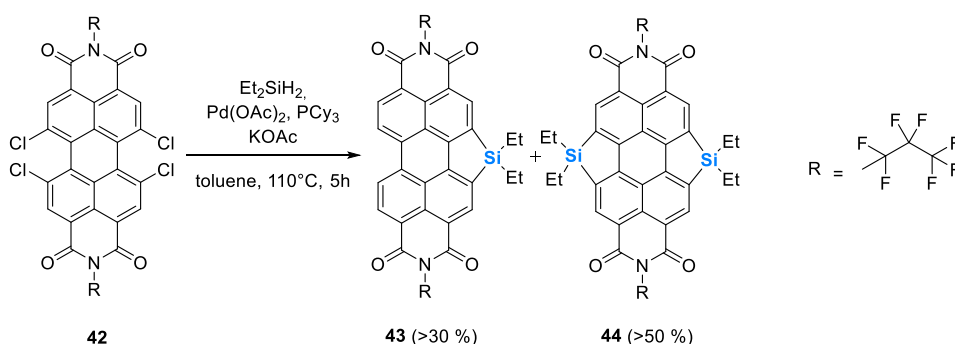


**Figure 6:** X-ray structures of **38** (a) and **41** (b)

In 2017, Ma *et al.* prepared the first sila- and disilaperylene diimides **43-44** (Scheme 7).<sup>45</sup> Such compounds were prepared through one pot Pd-catalysed Si-C bond

formation on tetrachloro-perylene diimide. The planarity of the perylene diimide core is not affected by the presence of the Si-rings. Of particular interest,  $\pi$ -stacking is observed in the structure of both compounds (average distance: 3.43 - 3.44 Å). As expected for perylene diimide derivatives **43-44** display intense absorption in the visible region ( $\lambda_{\text{abs}} = 540\text{-}550\text{ nm}$ ) accompanied by fluorescence with excellent quantum yields ( $> 88\%$ ) and very small Stokes shift ( $\sim 410\text{ cm}^{-1}$ ). The typical PDI-like two reversible reductions are observed without significant modulation compared to the non-silated analog ( $E_{\text{red}} \sim -0.90\text{ V vs Fc}^+/\text{Fc}$ ). To take advantage of the good electron affinity and favorable solid-state arrangement, crystalline sample of **43** and **44** were inserted in OFET showing efficient electron transport with mobility up to  $0.30\text{ cm}^2\cdot\text{V}^{-1}\cdot\text{s}^{-1}$  with on/off ratios of  $1.3 \cdot 10^5$ . Such excellent electron mobilities nicely illustrate that Si-containing PAHs can act as efficient n-type semi-conductors in optoelectronic devices.



### Scheme 7: Synthesis of silaperylenes diimides **43-44**

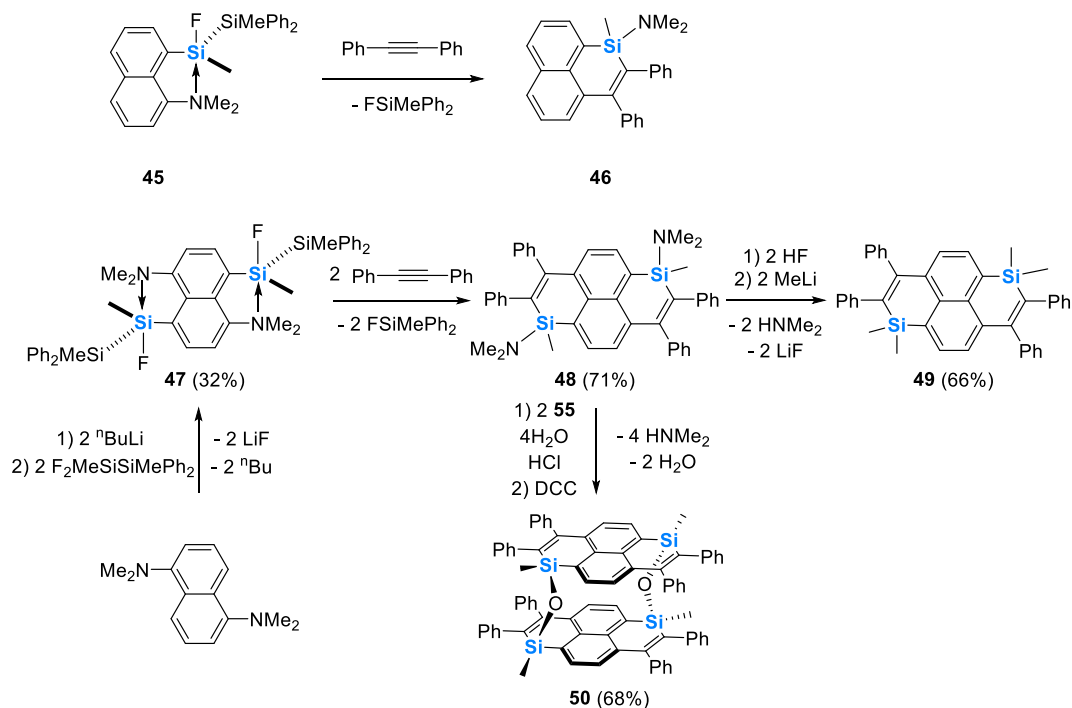
This section describes the synthesis of PAHs fused with group 14 metalloles. While the early compounds were prepared according to lithiation-substitution, the development of catalytic metalloles synthesis ( $\text{M} = \text{Pd}, \text{Rh}$ ) allowed diversifying the structures to obtain heteroatom-containing sumanenes, perylenes or [8]circulenes. All compounds feature the classical metalloles  $\sigma^*-\pi^*$  interactions or spiro conjugation which affect their optical and redox properties. However, the effect of changing the tetrel (Si to Ge to Sn) has only a limited impact on these properties, which is rather surprising given, for example, the tremendous impact of P-environment on phosphole-based PAHs.<sup>10a</sup>

## II. PAHs containing 6-membered heterocycles

Contrary to metalloles, there are limited example of  $\pi$ -conjugated 6-membered rings featuring heavy group 14 elements in the literature, mainly due to synthetic reasons. The presence of PAHs featuring those elements are thus even more limited. However, as we will see in this part, the development of catalytic methods recently allowed this field to rise quickly.

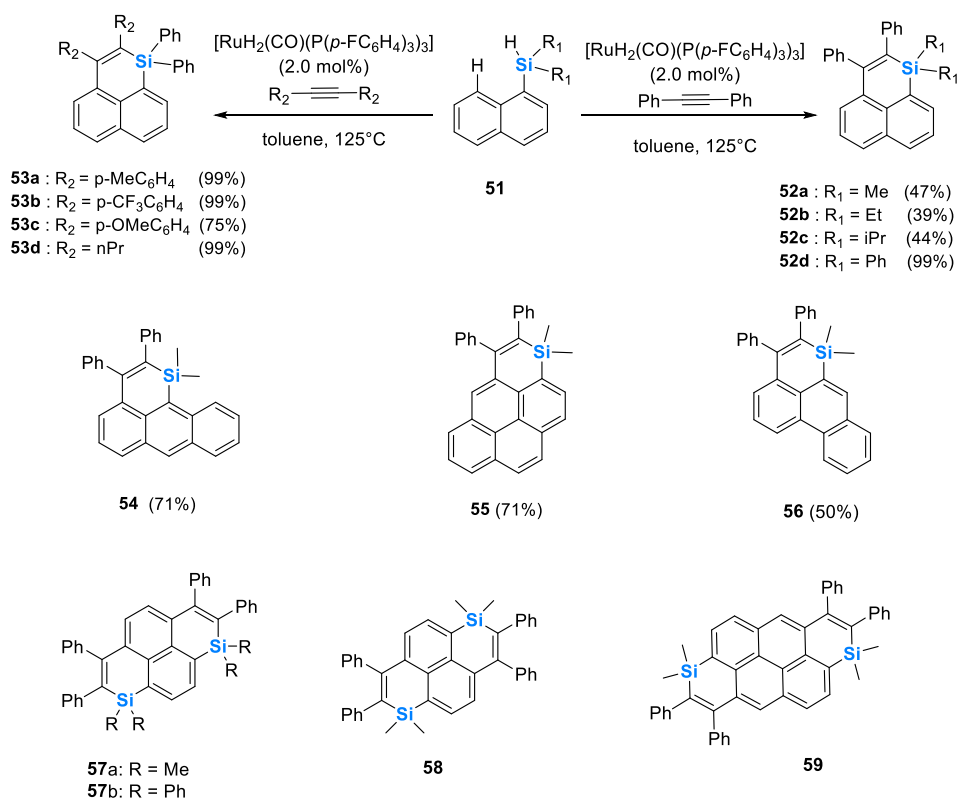
In 2000, Tamao and coworkers described the synthesis of silaphenalene **46** from pentacoordinate fluorodisilanes **45** through an ammonium sila-ylide intermediate (Scheme 8).<sup>46</sup> The authors postulate that the reaction proceeds through a complex mechanism involving silylene trapping with two acetylenes together with an amino migration to the Si atom. Later, the same team adapted this strategy for the

preparation of disilapyrene **49** (Scheme 8).<sup>47</sup> Interestingly, the authors could prepare the cage-like cyclophane dimer **50** by hydrolysis of intermediate **48** followed by dehydro-condensation. Both monomer and dimer display a planar polyaromatic framework. The photophysical properties of both “monomeric” **49** and dimer **50** were characterized. While **49** display a pyrene like UV-vis absorption at  $\lambda_{\text{abs}} = 394 \text{ nm}$ ,<sup>48</sup> dimer **50** features an additional red-shifted transition of low intensity ( $\lambda_{\text{abs}} = 412 \text{ nm}$ ). Dimer emission ( $\lambda_{\text{abs}} = 488 \text{ nm}$ ) is also red-shifted with a 10 fold increase in quantum yield compared to the monomer ( $\phi(\mathbf{50}) = 8\%$ ) and display the typical broad shape associated with pyrene excimer.



**Scheme 8:** Synthesis of silaphenalene **46**, disilaphenalene monomer **49** and dimer **50**.

In 2015, Fukuzawa and coworkers developed a Ru-catalysed approach toward silaphenalenes (Scheme 9).<sup>49</sup> This reaction consists of an annulation of 1-naphthylsilanes with alkynes catalysed by  $\text{RuH}_2(\text{CO})(\text{P}(\text{p-FC}_6\text{H}_4)_3)_3$ , proceeding through the cleavage of a C-H bond. It is tolerant to various naphthyl platform, silanes (**52**) and alkyne **53** (electron rich or electron poor). Such strategy is efficient and tolerant to many functional groups. Furthermore, it remains efficient with commercially available  $\text{RuH}_2(\text{CO})(\text{PPh}_3)_3$  as catalyst. One important factor is that such heterocycle synthesis does not involve  $^t\text{BuLi}$  in the last step contrary to many metalloles synthesis and is thus compatible with the introduction of many chemical functions. This methodology was used by Oyama’s team to prepare with good yields  $\pi$ -extended version of these silaphenalenes (**54-56**, Scheme 9) using the commercial catalyst.<sup>50</sup> X-ray crystallography confirmed that these compounds are fully planar. The UV-vis absorption and emission of the compounds were recorded and compared to their silane precursors. As expected, the annulation lead to a red-shift both in absorption and emission. All compounds are fluorescent both in diluted solution and in solid-state with quantum yields between 10% and 40%.



**Scheme 9:** Synthesis of sila- and disilaphenalenenes **52-59**

Finally, we also used this strategy to prepare a novel family of PAHs featuring two heteroatoms in the scaffold with various  $\pi$ -extension and Si-substituents (**57-59**, Scheme 9).<sup>51</sup> All those systems remain planar according to X-ray crystallography and DFT. Contrary to what was observed on simpler silaphenalenenes such **53**, the double annulation strategy did not allow introducing functional groups on the alkyne. Importantly, the absorption of disilapyrenes **57-58** (395 nm <  $\lambda_{\text{abs}}$  < 404 nm) is strongly redshifted from pyrene ( $\lambda_{\text{abs}} = 338$  nm). Accordingly, even if the delocalized  $\pi$ - $\pi^*$  transition has limited Si contributions according to TD-DFT, the electronic distribution strongly differs from pyrene<sup>48</sup> and the redshift is reproduced (Fig. 7). In our comprehensive structure-property relationships study, we observed that the size of the  $\pi$ -system has a moderate effect on the absorption ( $\Delta\lambda_{\text{abs}}(\mathbf{57a-59}) = 9$  nm). The luminescence in solution (DCM,  $c = 10^{-5}$  M) can however be finely tuned taking in consideration both the size of the  $\pi$ -system and the exocyclic substituents as the emission ( $\Delta\lambda_{\text{abs}}(\mathbf{57b-59}) = 66$  nm). The redox properties are also tunable as the use of more  $\pi$ -extended **59** ( $E_{\text{ox}} = +0.83$  V vs Fc<sup>+</sup>/Fc) or richer exocyclic group at the Si (Me / **57a** ( $E_{\text{ox}} = +0.88$  V vs Fc<sup>+</sup>/Fc) vs Ph / **57b** ( $E_{\text{ox}} = +0.95$  V vs Fc<sup>+</sup>/Fc) allows reducing the oxidation potential. Taking advantage of the solid-state luminescence of these derivatives, associated with suitable redox properties and thermal stability ( $T_{\text{d}10} = 411^\circ\text{C}$ ), we prepared multilayered fluorescent OLEDs using **57b** as dopant in two commercial host matrices, either through vacuum deposition or solution process. The devices display modest performances (maximal External Quantum Efficiency (EQE) = 1.5 %).<sup>52</sup> However, such performances may be ameliorated upon device engineering or by screening other host matrices, which paves the way toward the preparation of electroluminescent devices with enhanced properties.

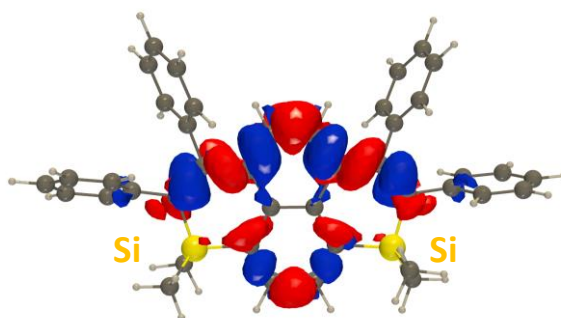
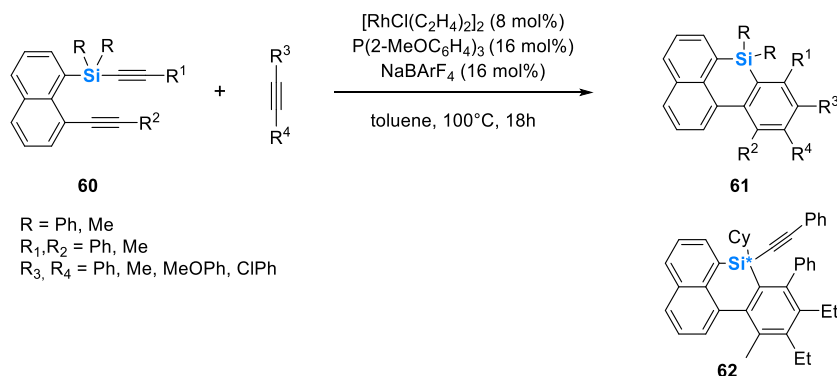


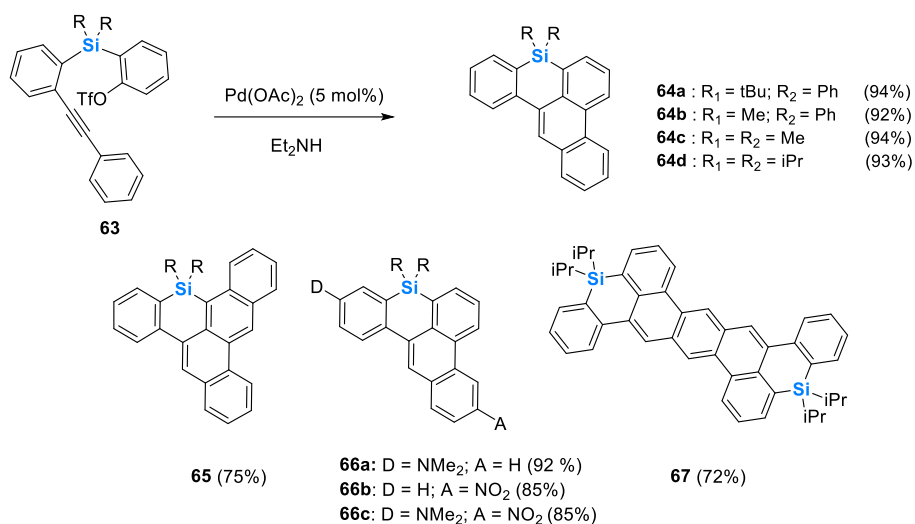
Figure 7: Electron density difference computed for **57a** (Blue / red regions respectively represent the decrease / increase of electron density upon absorption). Reprinted with permission from ref 51.

Recently, Shintani's research group developed two new catalytic methods to prepare PAHs containing 6-membered Si-cycles. The first method involves the preparation of benzonaphthosilines **61** through [2+2+2] cycloaddition catalysed by  $[\text{RhCl}(\text{C}_2\text{H}_4)_2]_2$  (Scheme 10).<sup>53</sup> The reaction is tolerant to various substituents on the silane or on the alkyne involved in the annulation (electron rich/ electron poor). The optical properties were briefly examined and moderate blue fluorescence both in solution ( $1\% < \phi < 20\%$ ) and in solid-state was reported ( $10\% < \phi < 20\%$ ). Investigation of an asymmetric version with a chiral phosphine as ligand illustrates that this reaction allows preparing compounds with stereogenic Si with promising enantioselectivity (ee = 80% for **62**, Scheme 10).



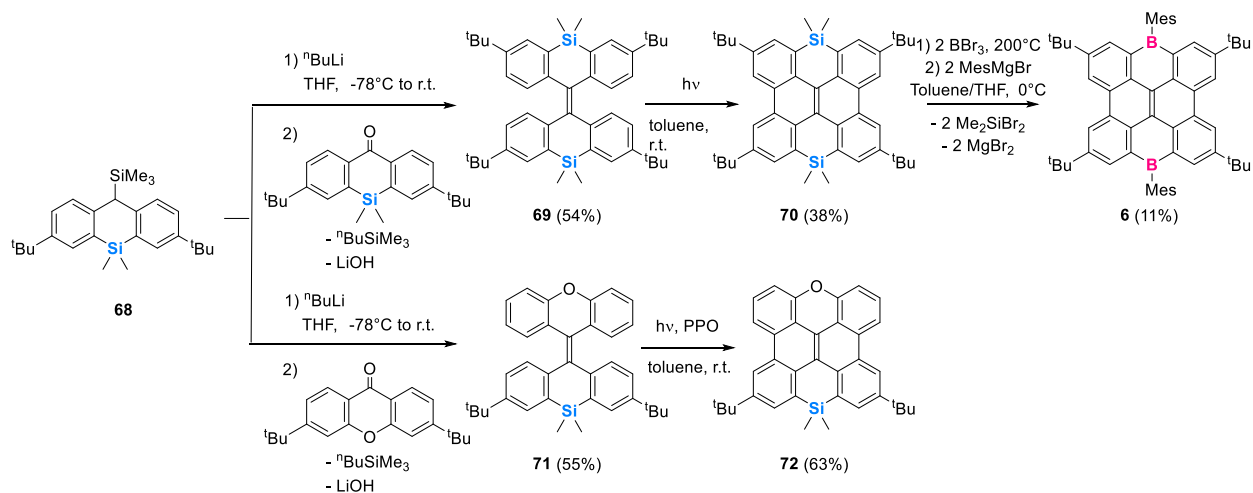
**Scheme 10:** Rh-catalysed access to benzonaphthosilines **61-62**

Shintani's team also developed a Pd-catalysed method to prepare benzophenanthrosilines **64** in good to excellent yields (> 72%, Scheme 11).<sup>54</sup> The proposed mechanism involves a C-H/C-H coupling through Pd migration and alkene stereoisomerization. The scope of the reaction is rather broad as it is compatible with different silanes (**64a-d**), different  $\pi$ -platforms (**65**) and with the introduction of electron-rich/electron poor substituents (**66**). It also allows the preparation of PAHs featuring two Si-cycles (**67**). The X-ray structure reveals that the  $\pi$ -platform is slightly distorted from planarity. Examination of the UV-vis/emission spectra illustrates that the optical properties of these benzophenanthrosilines can be effectively tuned in the visible range by modifying the substituents. Without surprise, insertion of electron-donating D group at the 10-position (**66a**) or electron-accepting A group at 3-position (**66b**) or both (**66c**) led to red-shifted absorption and emission.



### Scheme 11: Synthesis of benzophenanthrosilines **64-67**

In 2015, Wagner's group prepared boron-containing PAH **6** (Fig. 1 and Scheme 12).<sup>8,55</sup> A key compound in this procedure was the disilabisanthene **70** which was prepared through Peterson olefination followed by photocyclization. Contrary to **6** which is nearly planar, **70** displays a negative  $\pi$ -curvature (saddle-shape, see Fig. 8) as illustrated by its X-ray structure. Again, the average C-Si distance ( $d_{\text{C-Si}} = 1.85 \text{ \AA}$ , while the average  $d_{\text{C-B}} = 1.55 \text{ \AA}$ ) imposes some steric congestion. **70** absorbs and emit in the blue with an excellent quantum yield ( $\lambda_{\text{em}} = 408 \text{ nm}$ ,  $\phi = 70\%$ ). It also displays reversible oxidation (while the bora-analogues also display reversible reductions, as expected for tricoordinated boron-based  $\pi$ -systems).



### Scheme 12: Synthesis of sila- and disilabisanthene **70** and **72**?

In their study of multiple heteroatom doped bisanthenes, the same team prepared compound **72**, featuring Si and O atoms in the scaffold (Scheme 12).<sup>56</sup> This time, the  $\pi$ -platform is nearly planar (Fig. 8). Indeed, the steric congestion is released by the presence of short C-O bonds (average distances:  $d = 1.37 \text{ \AA}$ ) in the polycyclic skeleton. The fluorescence in solution is red-shifted compared to **70** due to the presence of electron rich O atom.

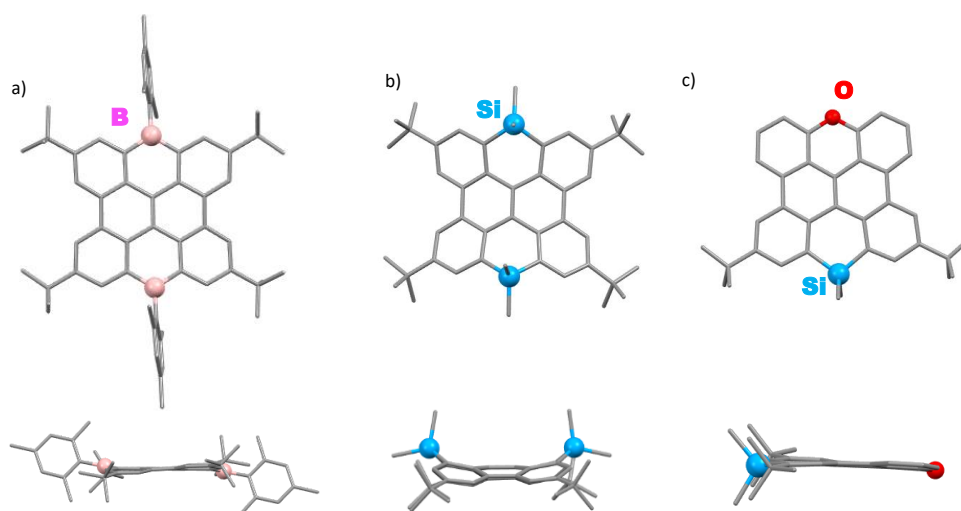
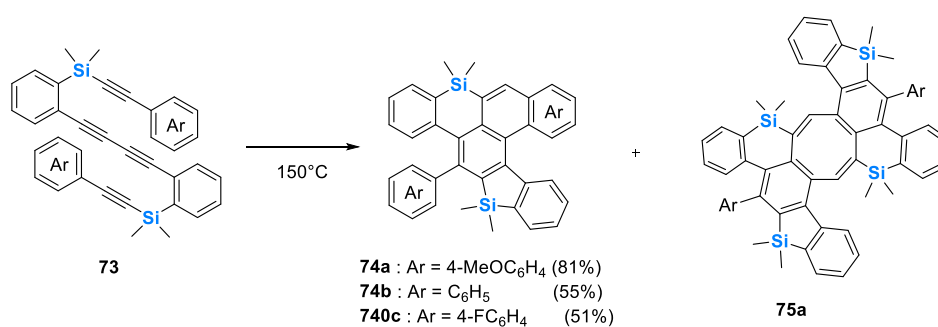


**Figure 8:** X-ray structures of **6** (a), **70** (b) and **72** (c)

Mitake *et al* described a sequence of hexadehydro-Diels–Alder followed by tetrahydro-Diels–Alder reactions of silicon-tethered tetraynes **73** to give PAHs featuring a 5-membered Si-cycle and a 6-membered Si-cycle **74** in moderate to excellent yield (81% for **74a**, Scheme 13).<sup>57</sup> The reaction scope is rather large as electron-rich and electron poor aryls could be used. The structure of **74a** reveals an helical  $\pi$ -framework imposed by the [5]helicene fragment (Fig. 9). Interestingly, a [2 + 2 + 2 + 2] cycloaddition by-product **75a** could be characterized and an optimized yield of 49% was obtained. This was the first example of a thermal [2 + 2 + 2 + 2] cycloaddition of alkynes for the preparation of  $\pi$ -conjugated eight-membered rings. The X-ray structure reveals a complex saddle-shaped  $\pi$ -framework (Fig. 9). All helicenoïd derivatives **74a-c** are luminescent in solution and in solid state. Substitution does not affect their absorption/emission properties.



**Scheme 13:** Dehydro-Diels-Alder approach to **74a-c** and **75a**



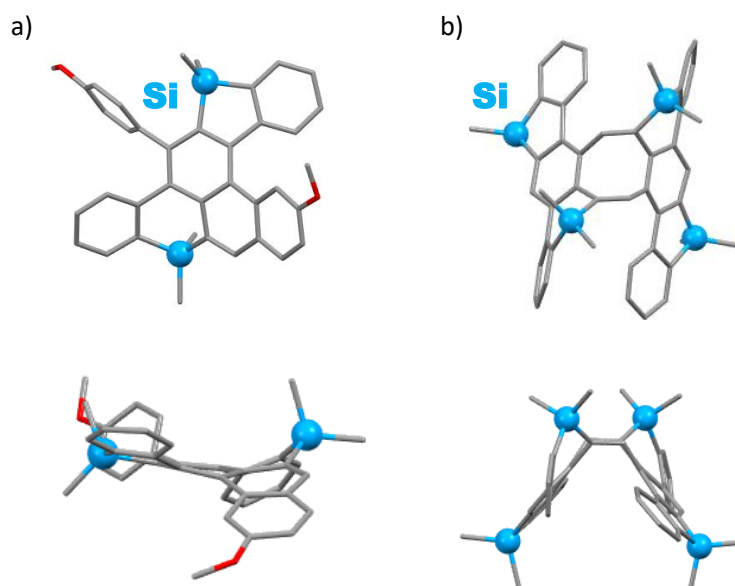


**Figure 9:** a) X-ray structure of **74a** and b) X-ray structure of **75a** (exocyclic aryl omitted for clarity)

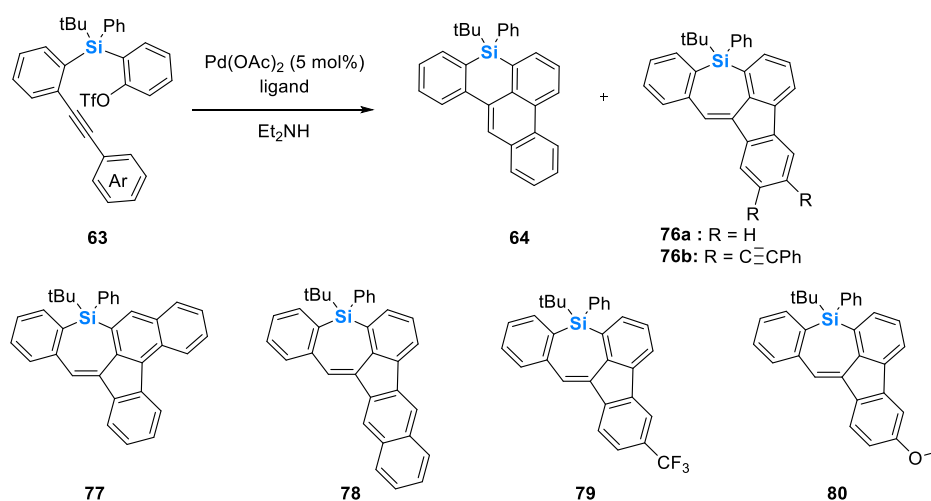
The field of PAHs featuring 6-membered Si-heterocycles recently developed thanks to the development of innovative catalytic approaches ( $M = \text{Pd}, \text{Ru}, \text{Rh}$ ) including C-H bond activation, as well as hexadehydro-Diels–Alder. Such methods allowed preparing fluorescent compounds that could be inserted into OLEDs. A step further in this field could be to implement these catalytic approaches to Ge as it has been done with 5-membered rings. Concerning Sn-based systems, the high reactivity of Sn-C bond, in particular in cross-coupling reactions, is clearly a limitation.

### III. PAHs containing 7-membered heterocycles

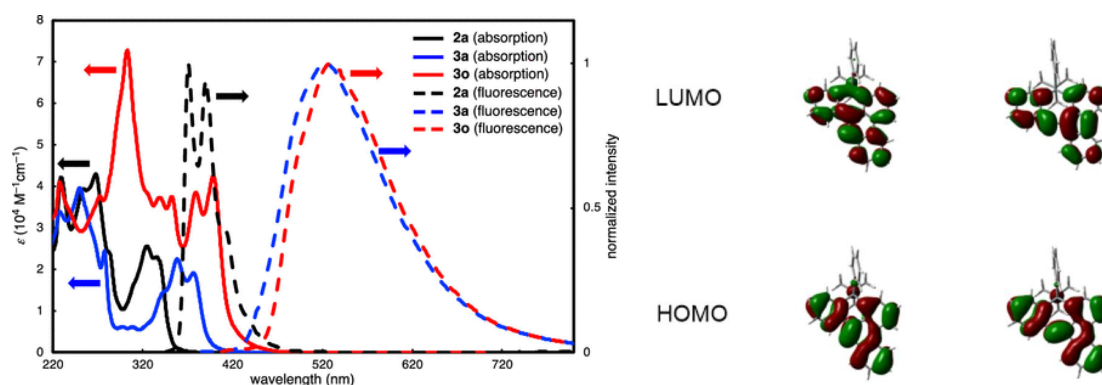
The development fully-carbonated  $\pi$ -systems featuring 7-membered rings is currently in fast development.<sup>58</sup> In contrast, the development of heteroatom containing 7-membered unsaturated heterocycles was limited due to fast rearomatization into aryl derivative.<sup>59</sup> However, the presence of substituents on the heteropine recently allowed stabilizing them and could lead to their insertion into functional materials.<sup>60</sup>

Regarding polyaromatic silepines, Shintani's research group recently reported that tuning the Pd catalyst (using of bisphosphine ligands possessing a biaryl scaffold) led to the preparation of benzofluorenosilepine **76** instead of benzophenanthrosilines **64** (Scheme 14).<sup>61</sup> Under optimal conditions (with BINAP (2,2'-Bis(diphenylphosphino)-1,1'-binaphthalene) as ligand), **76a** could be obtained in 67% yields. The proposed mechanism involves a 1,5-palladium migration followed by anti-carbopalladation of alkyne. As observed with related heteropines, the 7-membered cycle of **76a** displays boat shape structure. Various silanes, aromatic platforms (**77-78**) or functional groups (for example electron rich or electron poor such **79-80**) could be introduced. Importantly, preliminary tests with enantiopure (R)-BINAP leads to promising enantioselectivity (60% ee). Compared to **64** ( $\lambda_{\text{abs}} = 336 \text{ nm}/\lambda_{\text{em}} = 371 \text{ nm}$ ), **76a** displays a red-shifted absorption ( $\lambda_{\text{abs}} = 376 \text{ nm}$ ) and emission ( $\lambda_{\text{em}} = 523 \text{ nm}$ ) in DCM ( $c = 5 \cdot 10^{-5} \text{ M}$ ) (Fig. 10). This red-shift was attributed to a lower LUMO level, as evidenced by cyclic voltammetry ( $E_{\text{red}}(\mathbf{76a}) = -2.05 \text{ V}$  vs  $\text{Fc}^+/\text{Fc}$ , reversible wave, which is more positive by 0.20 V compared to the irreversible

reduction of **64**) and corroborated by DFT computations (Fig. X). In addition, while the HOMOs have similar shapes and energy, the electronic distribution strongly differs between **64** and **76a**. Furthermore, the modification of the  $\pi$ -platform allows fine-tuning the optical/redox properties of the silepines as observed in Fig. 10 with the red-shift between **76a** and **76b** due to  $\pi$ -extension.

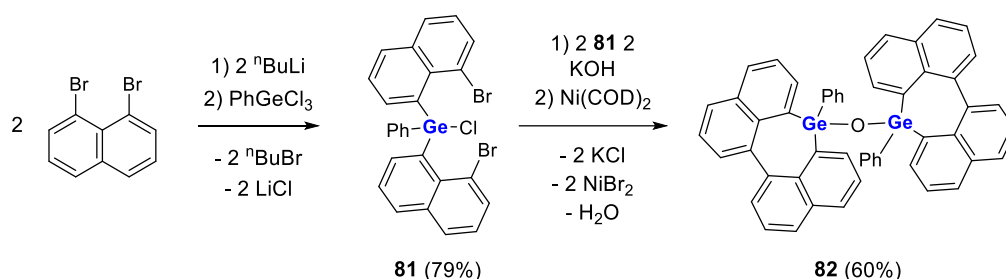


**Scheme 14:** Synthetic access to benzofluorenosilepines **76-80**



**Figures 10:** absorption/emission of **76a**, **76b** and **64** (respectively noted 3a, 3o and 2a in the scheme and FMOs of **64** (left) and **76a** (right)). Reprinted with permission from ref 61.

During our research on naphthyl-fused heteropines,<sup>62</sup> we prepared a dimer of naphthyl-fused germepine **82** through a Yamamoto coupling as the fusing step.<sup>63</sup> This compound displays absorption / emission in the blue range. Compared to its B and P-analogues, **82** displays a blue shifted absorption and higher Stokes shift. Such behaviour comes from the longer Ge-C bonds that make the polyaromatic scaffold less planar and rigid.



**Scheme 15:** Synthesis of naphthyl-fused germepine **82**.

While the field of PAHs featuring 7-membered rings is clearly rising, there are only limited examples of such derivatives with Si or Ge. However, the prepared compounds display interesting luminescent properties which should trigger the development of novel synthetic approaches to fully explore the potential of these novel  $\pi$ -systems.

#### IV. Conclusions

This review aims to shed light on the synthetic strategies to access PAHs featuring heavy group 14 elements (Si, Ge and Sn) and their optical and redox properties. As presented, a great diversity of structure has already been prepared with 5, 6 or 7-membered heterocycles and organotetrels including Si, Ge and Sn. While the first PAHs were prepared using lithiation-substitution, innovative synthetic approaches have been developed including Sila-Friedel-Crafts, metal catalysed approaches (Rh, Pd) or hexadehydro-Diels–Alder. This allowed to greatly diversify this family of derivatives. Even if changing the nature of the group heavy 14 element does not strongly impact its optical/redox properties, depending on the structure, the optical (absorption/emission) properties of the compounds could be tuned all over the visible spectral region, and their redox potential could be finely tuned. Some particular properties of the tetrels such as longer bond lengths than their C-counterparts or their ability to form spiro-derivatives could be used to tune both structures and properties. Finally, various examples of insertion into opto-electronic devices such as OFETs or OLEDs nicely illustrate that these derivatives will soon play a role in the field of optoelectronic devices. However, following the fast development of both PAHs and main-group chemistry, many challenges remain to be addressed by combining these two domains such as (i) the preparation of larger nanoribbons based on these structures<sup>64</sup> (ii) the incorporation of group-14 elements with unconventional valence (such as hyperconjugation or Si=C bonds) into PAHs,<sup>25,26</sup> (iii) the preparation of room-temperature phosphorescent compounds taking advantage of the presence of heavy main group elements<sup>65</sup> (iv) the study and optimization of the chiroptical properties of chiral compounds (the so-called chiral nanographenes or PAH featuring stereogenic tetrels), (v) stabilization of mono- and polyradical structures<sup>66</sup> (vi) the preparation of optimized opto-electronic devices.

#### II. Conflicts of interests

No conflict of interests.

### III. Acknowledgements

This work is supported by the Ministère de la Recherche et de l'Enseignement Supérieur, the CNRS, the Région Bretagne, the French National Research Agency (ANR Heterographene ANR-16-CE05-0003-01).

### IV. References

ORCID ID for authors: P-A Bouit: 0000-0002-0538-9276, M. Hissler: 0000-0003-1992-1814, T. Delouche: 0000-0002-5035-3010

---

<sup>1</sup> a) M. D. Watson, A. Fechtenkotter, K. Müllen, Big Is Beautiful—"Aromaticity" Revisited from the Viewpoint of Macromolecular and Supramolecular Benzene Chemistry, *Chem. Rev.* 101 (2001) 1267-1300, <https://doi.org/10.1021/cr990322p>; b) J. S. Wu, W. Pisula, K. Müllen, Graphenes as Potential Material for Electronics, *Chem. Rev.* 107 (2007) 718-747, <https://doi.org/10.1021/cr068010r>.

<sup>2</sup> A. Narita, X. Y. Wang, X. Feng, K. Müllen, New advances in nanographene chemistry, *Chem. Soc. Rev.* 44 (2015) 6616-6643, <https://doi.org/10.1039/C5CS00183H>.

<sup>3</sup> A. Narita, X. Feng,; Y. Hernandez, S. A. Jensen, M. Bonn, H. Yang, I. A. Verzhbitskiy, C. Casiraghi, M. R. Hansen, A. H. R. Koch, G. Fytas, O. Ivasenko, B. Li, K. S. Mali, T. S. Balandina, S. Mahesh, S. De Feyter, K. Müllen, Synthesis of structurally well-defined and liquid-phase-processable graphene nanoribbons, *Nat. Chem.* 6 (2014) 126-132, <https://doi.org/10.1038/nchem.1819>.

<sup>4</sup> K. Kawasumi, Q. Zhang, Y. Segawa, L. T. Scott, K. Itami, A grossly warped nanographene and the consequences of multiple odd-membered-ring defects, *Nat. Chem.* 5 (2013) 739-744, <https://doi.org/10.1038/nchem.1704>.

<sup>5</sup> Z. Qiu, S. Asako, Y. Hu, C. W. Ju, T. Liu, L. Rondin, D. Schollmeyer, J. S. Lauret, K. Müllen, A. J. Narita, Negatively Curved Nanographene with Heptagonal and [5]Helicene Units, *J. Am. Chem. Soc.* 142 (2020) 14814–14819, <https://doi.org/10.1021/jacs.0c05504>.

<sup>6</sup> A. Konishi, Y. Hirao, M. Nakano, A. Shimizu, E. Botek, B. Champagne, D. Shiomi, K. Sato, T. Takui, K. Matsumoto, H. Kurata, H. T. Kubo, Synthesis and Characterization of Teranthene: A Singlet Biradical Polycyclic Aromatic Hydrocarbon Having Kekulé Structures, *J. Am. Chem. Soc.* 132 (2010) 11021-11023, <https://doi.org/10.1021/ja1049737>

<sup>7</sup> a) M. Stępień, E. Gońka, M. Żyła, N. Sprutta, Heterocyclic Nanographenes and Other Polycyclic Heteroaromatic Compounds: Synthetic Routes, Properties, and Applications, *Chem. Rev.* 117 (2016) 3479–3716, , <https://doi.org/10.1021/acs.chemrev.6b00076>; b) A. Borisso, Y. K. Maurya, L. Moshniaba, W.-S. Wong, M. Zyla-Karwowska, M. Stępień, Recent Advances in Heterocyclic Nanographenes and Other Polycyclic Heteroaromatic Compounds, *Chem. Rev.* (2022), <https://doi.org/10.1021/acs.chemrev.1c00449>

- 
- <sup>8</sup> a) Z. Zhou, A. Wakamiya, T. Kushida, S. Yamaguchi, Planarized Triarylboranes: Stabilization by Structural Constraint and Their Plane-to-Bowl Conversion, *J. Am. Chem. Soc.* 134, (2012) 4529-4532, <https://doi.org/10.1021/ja211944q>; b) V. M. Hertz, M. Bolte, H.-W. Lerner, M. Wagner, Boron-Containing Polycyclic Aromatic Hydrocarbons: Facile Synthesis of Stable, Redox-Active Luminophores, *Angew. Chem. Int. Ed.*, 54 (2015) 8800-8804, <https://doi.org/10.1002/anie.201502977>.
- <sup>9</sup> S. M. Draper, D. J. Gregg, R. Madathil, Heterosuperbenzenes: A New Family of Nitrogen-Functionalized, Graphitic Molecules, *J. Am. Chem. Soc.* 124 (2002) 3486-3487, <https://doi.org/10.1021/ja017394u>.
- <sup>10</sup> a) P.-A. Bouit, A. Escande, R. Szűcs, D. Szieberth, C. Lescop, L. Nyulászi, M. Hissler, R. Réau, Dibenzophosphapentaphenes: Exploiting P Chemistry for Gap Fine-Tuning and Coordination-Driven Assembly of Planar Polycyclic Aromatic Hydrocarbons, *J. Am. Chem. Soc.* 134, (2012), 6524-6527, <https://doi.org/10.1021/ja300171y>; b) R. Szűcs, P.-A. Bouit, L. Nyulászi, M. Hissler, Phosphorus-Containing Polycyclic Aromatic Hydrocarbons, *ChemPhysChem* 18 (2017) 2618-2630, <https://doi.org/10.1002/cphc.201700438>.
- <sup>11</sup> L. Đorđević, C. Valentini, N. Demitri, C. Mézière, M. Allain, M. Sallé, A. Folli, D. Murphy, S. Mañas-Valero, E. Coronado, D. Bonifazi, O-Doped Nanographenes: A Pyrano/Pyrylium Route Towards Semiconducting Cationic Mixed-Valence Complexes, *Angew. Chem. Int. Ed.*, 59 (2020), 4106-4114, <https://doi.org/10.1002/anie.201914025>.
- <sup>12</sup> X. Feng, J. Wu, M. Ai, W. Pisula, L. Zhi, J. P. Rabe, K. Müllen, Triangle-Shaped Polycyclic Aromatic Hydrocarbons, *Angew. Chem. Int. Ed.* 46 (2007) 3033-3036, <https://doi.org/10.1002/ange.200605224>.
- <sup>13</sup> E. Hupf, Y. Tsuchiya, W. Moffat, L. Xu, M. Hirai, Y. Zhou, M. J. Ferguson, R. McDonald, T. Murai, G. He, E. Rivard, A Modular Approach to Phosphorescent  $\pi$ -Extended Heteroacenes, *Inorg. Chem.* 58 (2019), 13323-13336
- <sup>14</sup> a) T. Baumgartner, F. Jaekle (Eds.), *Main Group Strategies toward Functional Hybrid Materials*, John Wiley & Sons, UK, 2018; b) E. Hey-Hawkins, M. Hissler (Eds.), *Smart Inorganic Polymers*, John Wiley & Sons, UK, 2019.
- <sup>15</sup> M. Hissler, P. W. Dyer, R. Réau, Linear organic  $\pi$ -conjugated systems featuring the heavy Group 14 and 15 elements, *Coord. Chem. Rev.* 244 (2003) 1-44, [https://doi.org/10.1016/S0010-8545\(03\)00098-5](https://doi.org/10.1016/S0010-8545(03)00098-5).
- <sup>16</sup> S. Yamaguchi, K. J. Tamao, *Chem. Soc., Silole-containing  $\sigma$ - and  $\pi$ -conjugated compounds*, *Dalton Trans.* (1998) 3693-3702, <https://doi.org/10.1039/A804491K>.
- <sup>17</sup> Y. Hong, J. W. Y. Lam, B. Z. Tang, Aggregation-induced emission, *Chem. Soc. Rev.* 40 (2011) 5361-5388, <https://doi.org/10.1039/C1CS15113D>.
- <sup>18</sup> S. M. Parke, M. P. Boone, E. Rivard, Marriage of heavy main group elements with  $\pi$ -conjugated materials for optoelectronic applications, *Chem Commun.* 52 (2016) 9485-9505, <https://doi.org/10.1039/C6CC04023C>

- 
- <sup>19</sup> I.-M. Ramirez y Medina, M. Rohdenburg, F. Mostaghimi, S. Grabowsky, P. Swiderek, J. Beckmann, J. Hoffmann, V. Dorcet, M. Hissler, A. Staubitz, Tuning the Optoelectronic Properties of Stannoles by the Judicious Choice of the Organic Substituents, *Inorg. Chem.* 57 (2018) 20, 12562-12575, <https://doi.org/10.1021/acs.inorgchem.8b01649>.
- <sup>20</sup> T.-Y. Chu, J. Lu, S. Beaupré, Y. Zhang, J.-R. Pouliot, S. Wakim, J. Zhou, M. Leclerc, Z. Li, J. Ding, Y. Tao, Bulk Heterojunction Solar Cells Using Thieno[3,4-c]pyrrole-4,6-dione and Dithieno[3,2-b:2',3'-d]silole Copolymer with a Power Conversion Efficiency of 7.3%, *J. Am. Chem. Soc.* 133 (2011) 4250-4253, <https://doi.org/10.1021/ja200314m>.
- <sup>21</sup> C. M. Amb, S. Chen, K. R. Graham, J. Subbiah, C. E. Small, F. So, J. R. Reynolds, Dithienogermole As a Fused Electron Donor in Bulk Heterojunction Solar Cells, *J. Am. Chem. Soc.*, 133 (2011) 10062-10065, <https://doi.org/10.1021/ja204056m>.
- <sup>22</sup> a) L. G. Mercier, W. E. Piers, M. Parvez, Benzo- and Naphthoborepins: Blue-Emitting Boron Analogues of Higher Acenes, *Angew. Chem. Int. Ed.* 48 (2009) 6108-6111, <https://doi.org/10.1002/anie.200902803>; b) P. A. Chase, W. E. Piers, B. O. Patrick, New Fluorinated 9-Borafluorene Lewis Acids, *J. Am. Chem. Soc.* 122 (2000), 12911–12912, <https://doi.org/10.1021/ja005607u>.
- <sup>23</sup> M. Saito, M. Sakaguchi, T. Tajima, K. Ishimura, S. Nagase, Synthesis, Structures, and Properties of Plumboles, Phosphorus, Sulfur Silicon Relat. Elem. 185 (2010) 1068–1076, <https://doi.org/10.1080/10426501003773399>.
- <sup>24</sup> T. Kuwabara, M. Saito, Siloles, Germoles, Stannoles, and Plumboles, *Comprehensive Heterocyclic Chemistry IV*, 3 (2022), 798-832, <https://doi.org/10.1016/B978-0-12-409547-2.14789-4>
- <sup>25</sup> S. Yamaguchi, S. Akiyama, K. Tamao, Photophysical Properties Changes Caused by Hypercoordination of Organosilicon Compounds: From Trianthrylfluorosilane to Trianthryldifluorosilicate, *J. Am. Chem. Soc.* 122 (2000) 6793-6794, <https://doi.org/10.1021/ja001042q>.
- <sup>26</sup> B. Su, A. Kostenko, Y. Yao, M. Driess, Isolable Dibenzo[a,e]disilapentalene with a Dichotomic Reactivity toward CO<sub>2</sub>, *J. Am. Chem. Soc.* 142 (2020) 16935–16941, <https://doi.org/10.1021/jacs.0c09040>.
- <sup>27</sup> T. Nukazawa, T. Iwamoto, An Isolable Tetrasilicon Analogue of a Planar Bicyclo[1.1.0]butane with  $\pi$ -Type Single-Bonding Character, *J. Am. Chem. Soc.* 142 (2020) 9920-9924, <https://doi.org/10.1021/jacs.0c03874>.
- <sup>28</sup> a) A. Fukazawa, S. Yamaguchi, Ladder  $\pi$ -Conjugated Materials Containing Main-Group Elements, *Chem. As. J.* 4 (2009) 1386-1400, <https://doi.org/10.1002/asia.200900179>; b) K. Dhbaibi, L. Favereau, J. Crassous, Enantioenriched Helicenes and Helicenoids Containing Main-Group Elements (B, Si, N, P), *Chem. Rev.* 119 (2019) 8846-8953, <https://doi.org/10.1021/acs.chemrev.9b00033>. (.
- <sup>29</sup> a) T. A. Schaub, K. Padberg, M. Kivala, Bridged triarylboranes, -silanes, -amines, and -phosphines as minimalistic heteroatom-containing polycyclic aromatic hydrocarbons: Progress and challenges, *J. Phys. Org. Chem.* 33 (2020) 4022-4049, <https://doi.org/10.1002/poc.4022> ; b)

---

M. Hirai, N. Tanaka, M. Sakai, S. Yamaguchi, Structurally Constrained Boron-, Nitrogen-, Silicon-, and Phosphorus-Centered Polycyclic  $\pi$ -Conjugated Systems, *Chem. Rev.* 119 (2019) 8291–8331, <https://doi.org/10.1021/acs.chemrev.8b00637>

<sup>30</sup> Covalent radii from: P. Pyykkö, M. Atsumi, Molecular Single-Bond Covalent Radii for Elements 1–118, *Chem. Eur. J.* 15 (2009) 186–197, <https://doi.org/10.1002/chem.200800987>.

<sup>31</sup> S. Furukawa, J. Kobayashi, T. Kawashima, Development of a Sila-Friedel–Crafts Reaction and Its Application to the Synthesis of Dibenzosilole Derivatives, *J. Am. Chem. Soc.* 131 (2009) 14192–14193, <https://doi.org/10.1021/ja906566r>.

<sup>32</sup> S. Furukawa, J. Kobayashi, T. Kawashima, Development of a Sila-Friedel–Crafts Reaction and Its Application to the Synthesis of Dibenzosilole Derivatives, *Dalton Trans.* 39 (2010) 9329–9336, <https://doi.org/10.1021/ja906566r>.

<sup>33</sup> T. Tanikawa, M. Saito, J. D. Guo, S. Nagase, Synthesis, structures and optical properties of trisilasumanene and its related compounds, *Org. Biomol. Chem.*, 9 (2011) 1731–1735, <https://doi.org/10.1039/C0OB00987C>.

<sup>34</sup> Recent reviews on heterasumanenes: a) M. Saito, S. Furukawa, J. Kobayashi, T. Kawashima, The Chemistry of Heterasumanenes, *Chem. Rec.* 16 (2016) 64–72, <https://doi.org/10.1002/tcr.201500211>; b) W. Wang, X. Shao, Synthesis and derivatization of hetero-buckybowls, 19 (2021) 101–122, <https://doi.org/10.1039/D0OB01931C>.

<sup>35</sup> T. Tanikawa, M. Saito, J. D. Guo, S. Nagase, M. Minoura, Synthesis, Structures, and Optical Properties of Heterasumanenes Containing Group 14 Elements and Their Related Compounds, *Eur. J. Org. Chem.* (2012) 7135–7142, <https://doi.org/10.1002/ejoc.201201223>.

<sup>36</sup> M. Saito, T. Tanikawa, T. Tajima, J. D. Guo, S. Nagase, Synthesis and structures of heterasumanenes having different heteroatom functionalities, *Tetrahedron Lett.* 51 (2010) 672–675, <https://doi.org/10.1016/j.tetlet.2009.11.102>.

<sup>37</sup> D. Zhou, Y. Gao, B. Liu, Q. Tan, B. Xu, Synthesis of Silicon and Germanium-Containing Heterosumanenes via Rhodium-Catalyzed Cyclodehydrogenation of Silicon/Germanium–Hydrogen and Carbon–Hydrogen Bonds, *Org. Lett.* 19 (2017) 4628–4631, <https://doi.org/10.1021/acs.orglett.7b02254>.

<sup>38</sup> Q. Tan, D. Zhou, T. Zhang, B. Liu, B. Xu, Iodine-doped sumanene and its application for the synthesis of chalcogenasumanenes and silasumanenes, *Chem. Commun.* 53 (2017) 10279–10282, <https://doi.org/10.1039/C7CC05885C>.

<sup>39</sup> S. Furakawa, K. Hayashi, K. Yamagishi, M. Saito, Synthesis and properties of spiro-type heterasumanenes containing group 14 elements as bridging atoms, *Mater. Chem. Front.* 2 (2018) 929–934, <https://doi.org/10.1039/C7QM00590C>.

- 
- <sup>40</sup> T. Ohmae, T. Nishinaga, M. Wu, M. Iyoda, Cyclic Tetrathiophenes Planarized by Silicon and Sulfur Bridges Bearing Antiaromatic Cyclooctatetraene Core: Syntheses, Structures, and Properties, *J. Am. Chem. Soc.* **132** (2010) 1066–1074, <https://doi.org/10.1021/ja908161r>.
- <sup>41</sup> a) C. N. Feng, M.Y Kuo, Y.T Wu, Synthesis, Structural Analysis, and Properties of [8]Circulenes, *Angew. Chem. Int. Ed.* **52** (2013), 7791–7794, <https://doi.org/10.1002/anie.201303875>;  
b) Y. Sakamoto, T. Suzuki, Tetrabenzo[8]circulene: Aromatic Saddles from Negatively Curved Graphene, *J. Am. Chem. Soc.* **135** (2013), 14074–14077, <https://doi.org/10.1021/ja407842z>
- <sup>42</sup> Y. Miyake, H. Shinokubo, Hetero[8]circulenes: synthetic progress and intrinsic properties, *Chem Commun.* **56** (2020) 15605–15614, <https://doi.org/10.1039/D0CC06495E>.
- <sup>43</sup> Y. Serizawa, S. Akahori, S. Kato, H. Sakai, T. Hasobe, Y. Miyake, H. Shinokubo, Synthesis of Tetrasilatetrathia[8]circulenes by a Fourfold Intramolecular Dehydrogenative Silylation of C–H Bonds, *Chem. Eur. J.* **23** (2017) 6948–6952, <https://doi.org/10.1002/chem.201700729>
- <sup>44</sup> S. Akahori, H. Sakai, T. Hasobe, H. Shinokubo, Y. Miyake, Synthesis and Photodynamics of Tetragermatetrathia[8]circulene, *Org. Lett.* **20** (2018), 304–307, <https://doi.org/10.1021/acs.orglett.7b03764>
- <sup>45</sup> Z. Ma, C. Xiao, C. Liu, D. Meng, W. Jiang, Z. Wang, Palladium-Catalyzed Si–C Bond Formation toward Sila-Annulated Perylene Diimides *Org. Lett.* **19** (2017) 4331–4334, <https://doi.org/10.1021/acs.orglett.7b02011>.
- <sup>46</sup> T. Saeki, A. Toshimitsu, K. Tamao, Thermolysis of bis(pentacoordinate) silicon compound bearing two 1-fluorodisilanyl units at 4- and 8-positions on 1,5-bis(dimethylamino)naphthalene ring: construction of disilapyrene skeleton and cyclophane-shaped siloxane dimer, *J. Organomet. Chem.* **686**, (2003) 215–222, [https://doi.org/10.1016/S0022-328X\(03\)00376-0](https://doi.org/10.1016/S0022-328X(03)00376-0).
- <sup>47</sup> T. Saeki, A. Toshimitsu, K. Tamao, Thermolysis of bis(pentacoordinate) silicon compound bearing two 1-fluorodisilanyl units at 4- and 8-positions on 1,5-bis(dimethylamino)naphthalene ring: construction of disilapyrene skeleton and cyclophane-shaped siloxane dimer, *J. Organomet. Chem.* **686**, (2003) 215–222, [https://doi.org/10.1016/S0022-328X\(03\)00376-0](https://doi.org/10.1016/S0022-328X(03)00376-0).
- <sup>48</sup> A. G. Crawford, A. D. Dwyer, Z. Liu, A. Steffen, A. Beeby, L.-O. Pålsson, D. J. Tozer and T. B. Marder, Experimental and Theoretical Studies of the Photophysical Properties of 2- and 2,7-Functionalized Pyrene Derivatives, *J. Am. Chem. Soc.* **133** (2011), 13349–13362, [dx.doi.org/10.1021/ja2006862](https://doi.org/10.1021/ja2006862)
- <sup>49</sup> Y. Tokoro, K. Sugita, S. Fukuzawa, Synthesis of Silaphenalenenes by Ruthenium-Catalyzed Annulation between 1-Naphthylsilanes and Internal Alkynes through C–H Bond Cleavage, *Chem. Eur. J.*, **21** (2015) 13229–13232, <https://doi.org/10.1002/chem.201502746>.
- <sup>50</sup> Y. Tokoro, T. Oyama, Synthesis and Characterization of (Di)Benzosilaphenalenenes, *Chem. Lett.*, **47**, (2018) 130–133, <https://doi.org/10.1246/cl.170939>.
- <sup>51</sup> T. Delouche, G. Taifour, M. Cordier, T. Roisnel, D. Tondelier, P. Manzhi, B. Geffroy, B. Le Guennic, D. Jacquemin, M. Hissler, P.-A. Bouit, Si-containing Polycyclic Aromatic Hydrocarbons: Synthesis and Opto-electronic Properties, *Chem. Commun.* **58** (2022) 88–91, <https://doi.org/10.1039/D1CC06309J>.



---

<sup>52</sup> Such EQE should be compared to the limit of fluorescent emitters which is 5%, see: G. Hong, X. Gan, C. Leonhardt, Z. Zhang, J. Seibert, J. M. Busch, S. Bräse, A Brief History of OLEDs—Emitter Development and Industry Milestones *Adv. Mater.* 33 (2021), 2005630, <https://doi.org/10.1002/adma.202005630>

<sup>53</sup> T. Maesato, R. Shintani, Synthesis of 7H-Benzo[e]naphtho[1,8-bc]silines by Rhodium-catalyzed [2 + 2 + 2] Cycloaddition, *Chem. Lett.*, 49 (2020) 344–346, <https://doi.org/10.1246/cl.200025>.

<sup>54</sup> Tsuda, T.; Kawakami, Y.; S.-M. Choi, R. Shintani, Palladium-Catalyzed Synthesis of Benzophenanthrosilines by C–H/C–H Coupling through 1,4-Palladium Migration/Alkene Stereoisomerization, *Angew. Chem. Int. Ed.*, 59 (2020) 8057–8061, <https://doi.org/10.1002/ange.202000217>.

<sup>55</sup> V. M. Hertz, N. Ando, M. Hirai, M. Bolte, H. W. Lerner, S. Yamaguchi, M. Wagner, Steric Shielding vs Structural Constraint in a Boron-Containing Polycyclic Aromatic Hydrocarbon, *Organometallics*, 36 (2017) 2512–2519, <https://doi.org/10.1021/acs.organomet.6b00800>.

<sup>56</sup> V. M. Hertz, J. G.; Massoth, M. Bolte, H.-W. Lerner, M. Wagner, En Route to Stimuli-Responsive Boron-, Nitrogen-, and Sulfur-Doped Polycyclic Aromatic Hydrocarbons, *Chem. Eur. J.* 22 (2016) 13181-13188, <https://doi.org/10.1002/chem.201602406>.

<sup>57</sup> A. Mitake, R. Nagai, A. Sekine, H. Takano, N. Sugimura, K. S. Kanyiva, T. Shibata, Consecutive HDDA and TDDA reactions of silicon-tethered tetraynes for the synthesis of dibenzosilole-fused polycyclic compounds and their unique reactivity, *Chem. Sci.* 10 (2019) 6715-6720, <https://doi.org/10.1039/C9SC00960D>.

<sup>58</sup> C. Chaolumen, I. A. Stepek, K. E. Yamada, H. Ito, K. Itami, Construction of Heptagon-Containing Molecular Nanocarbons, *Angew. Chem. Int. Ed.* 60 (2021) 23508-23532, <https://doi.org/10.1002/anie.202100260>.

<sup>59</sup> a) H. Sakurai, K. Oharu, Y. Nakdaira, Preparation and Some Reactions of Dibenzo-7-silanorbornadiene Derivatives, *Chem. Lett.* 15 (1986) 1797-1800, <https://doi.org/10.1246/cl.1986.1797>; b) M. L. G. Borst, R. E. Bulo, D. J. Gibney, Y. Alem, F. J. J. de Kanter, A. W. Ehlers, M. Schakel, M. Lutz, A. L. Spek, K. Lammertsma, C., 3H-Benzophosphepine Complexes: Versatile Phosphinidene Precursors *J. Am. Chem. Soc.* 127 (2005), 127, 16985-16999. <https://doi.org/10.1021/ja054885>.

<sup>60</sup> L. Wang, J. Ma, E. Si, D. Zheng, Recent Advances in Luminescent Annulated Borepins, Silepins, and Phosphepins, *Synthesis* 53 (2020) 623-635, <https://doi.org/10.1055/s-0040-1705946>.

<sup>61</sup> T. Tsuda, S.-M. Choi, R. Shintani, Palladium-Catalyzed Synthesis of Dibenzosilepin Derivatives via 1,*n*-Palladium Migration Coupled with anti-Carbopalladation of Alkyne, *J. Am. Chem. Soc.* 143 (2021) 1641-1650, <https://doi.org/10.1021/jacs.0c12453>.

<sup>62</sup> T. Delouche, R. Mokrai, T. Roisnel, D. Tondelier, B. Geffroy, L. Nyulászi, Z. Benkő, M. Hissler, P.-A., Bouit, Naphthyl-fused phosphepines: Luminescent contorted polycyclic P-heterocycles, *Chem. Eur. J.*, 26 (2020) 1856 –1863, <https://doi.org/10.1002/chem.201904490>.

---

<sup>63</sup> T. Delouche, T. Roisnel, V. Dorcet, M. Hissler, P.-A. Bouit, Mixing Polyaromatic Scaffolds and Main Group Elements: Synthesis, Coordination and Optical Properties of Naphthyl-Fused Heteropines, *Eur. J. Inorg. Chem.* 11 (2021) 1082-1089, <https://doi.org/10.1002/ejic.202001097>.

<sup>64</sup> T. Marangoni, D. Haberer, D. J. Rizzo, R. R. Cloke, F. R. Fischer, Heterostructures through Divergent Edge Reconstruction in Nitrogen-Doped Segmented Graphene Nanoribbons, *Chem. Eur. J.* 22 (2016) 13037 – 13040, <https://doi.org/10.1002/chem.201603497>.

<sup>65</sup> S. M. Parke, E. Rivard, Aggregation induced phosphorescence in the main group, *Isr. J. Chem.* 58 (2018) 915-926, <https://doi.org/10.1002/ijch.201800039>.

<sup>66</sup> S. Honda, R. Sugawara, S. Ishida, T. Iwamoto, A Spiropentasiladiene Radical Cation: Spin and Positive Charge Delocalization across Two Perpendicular Si=Si Bonds and UV–vis–NIR Absorption in the IR-B Region, *J. Am. Chem. Soc.*, 143 (2021) 2649–2653, <https://doi.org/10.1021/jacs.0c12426>.